

## Characterizations of the Late Cenomanian Reservoirs, El Diyur Field, North Western Desert, Egypt

Esam A. El-Gawad<sup>1</sup>, Mohamed Fathy<sup>1</sup>, and Mohamed M.Ali<sup>2</sup>,

<sup>1</sup>Department of Geology, Faculty of Science, Al-Azhar University, Cairo, Egypt.

<sup>2</sup>Qarun Petroleum Company, (Apache J.V), Egypt.

**Abstract:** The study aimed to combine the different available data to understand the subsurface system and the characteristic of Late Cretaceous reservoirs in El Diyur field to represent the vertical and lateral heterogeneity at the well, multi-well, and field scale, which could be used as a tool for reservoir management. Seismic interpretation was conducted on the seismic sections that concerned the study area to make a detailed structural interpretation to determine the structural geometry of the Late Cretaceous horizons. Petrophysical well log analysis of the reservoir rock of Abu Roash “G-10” and “G-20” zones have been done and mapped. The estimated volume of Original Hydrocarbon in Place of Abu Roash “G-10” and “G-20” zones have been calculated.

### I. Introduction

El Diyur field is located in the north Western Desert of Egypt, between latitudes 29° 23' N- 29° 25' N and longitudes 29° 20' E- 29° 24' E occupying a current area of 27 square kilometers (Fig.1). El Diyur field lies on the southern eastern margin of Abu Gharadig Basin and west of East Bahariya Concession.

### II. Materials and methods

Interpretation was conducted on seismic lines and (GR, Resistivity, Density and Neutron) logs of four wells extracted from El-Diyur field (Fig.1). Integrated methods involving seismic interpretation and petrophysical data analysis were employed to meet the objectives of this study. Interpretations of seismic sections were done, Abu Roash “G-10” and “G-20” zones were identified and evaluated by generating various maps such as structural, net reservoir isopach, arithmetic average water saturation and arithmetic average effective porosity maps.

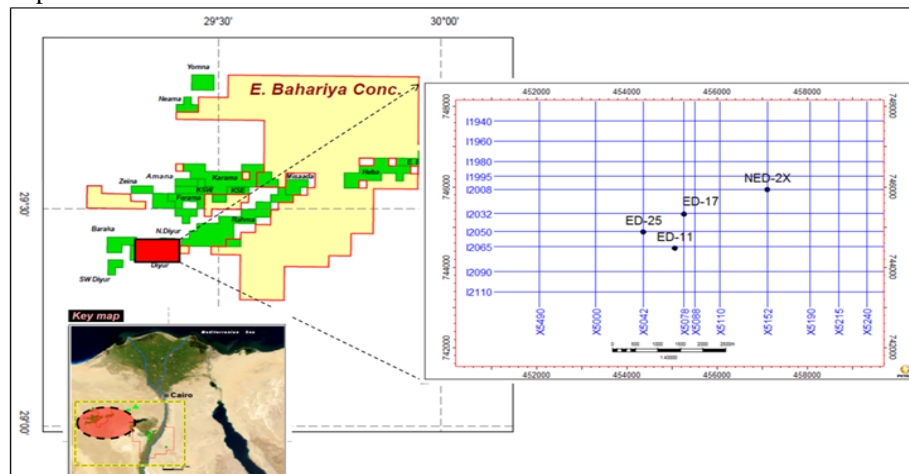


(Fig.1): Location map of El Diyur field north Western Desert, Egypt

### Geological Setting

#### Stratigraphic setting

The stratigraphic section of the North Western Desert is thick and includes most of the sedimentary succession from recent to Pre-Cambrian basement complex [1] (Fig.2). The sedimentary sequence of the study area based on deepest drilled well ranges in age from the Early Jurassic Ras Qattara Formation to Miocene Moghra Formation at surface. The Cretaceous mega-sequence is divided into Lower and Upper sequences, the Lower Cretaceous includes Alam El Bueib, Alamein, Dahab and Kharita formations while the Upper Cretaceous

sequence incorporates Bahariya, Abu Roash and Khoman formations [2]. The Late Cretaceous Abu Roash “G” Member represent the main reservoirs in the study area, it is a Late Cenomanian in age [3]. It is heterogeneous both vertically and laterally, and becomes sandy through Abu Gharadig basin [4]. In the study area Abu Roash “G” member consist of shale, limestone, sandstone, with siltstone streaks.

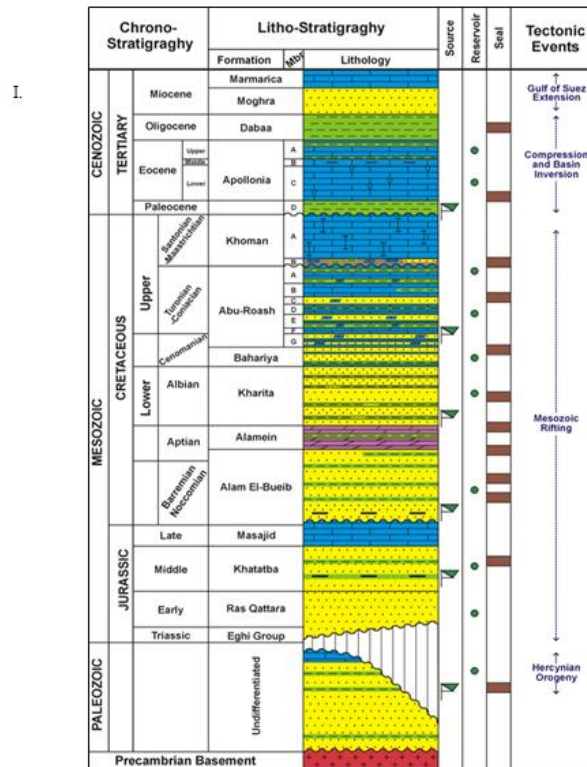


(Fig.2): Generalized stratigraphic column of the north Western Desert of Egypt. [5]

### Tectonic setting

The structural patterns in north Western Desert from the Late Jurassic to Early Tertiary appear to have been influenced significantly by two primary tectonic forces related to Tethyan plate tectonics: (1) the sinistral shear during the Late Jurassic to Early Cretaceous and (2) the dextral shear during the Late Cretaceous to Paleocene time [6]. Interpreted seismic section (x-line 5152) was selected in order to illustrate the picking of horizons and structure features in the study area. This section shows seven seismic reflectors were picked (Upper Bahariya Formation, Abu Roash "G" Member, Abu Roash "G20", Abu Roash "G-15" zones, Abu Roash "D", Abu Roash "A", members, Khoman and Apollonia formations).

### North-South trending seismic section (5152):

This seismic section was oriented to the N-S direction of the study area (Fig.3) passing through North El Diyur-2X well. Late Cretaceous reflectors seem to be parallel, semi parallel and gradually dipping toward the north. East-West trending major normal fault (F1) which dip toward the south influences the Late Cretaceous sequence (Upper Bahariya and Abu Roash formations) and older unites with vertical relief more than the western part of the field. This fault also influences on top of Khoman and Apollonia formations which less deformed than the older Bahariya and Abu Roash formations, the fault terminates at base Dabaa Formation. A lateral variation of Khoman thickness observed, Khoman is thicker in the down thrown side which reflects a large accommodation space on the down thrown side of the major normal fault (F1) which indicates that the major normal fault (F1) is a syn-depositional fault at time of Khoman deposition (Late Santonian to Maasterchitian age).

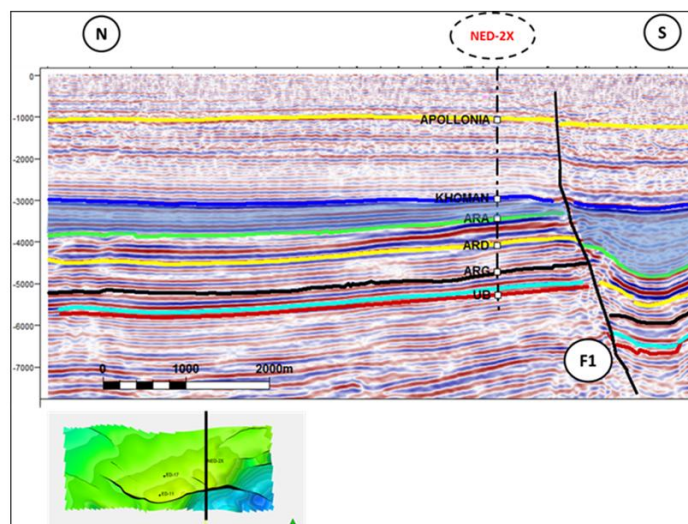


(Fig. 1): N-S trending seismic section (5152) passing through NED-2X well.

### Structure contour maps

Structure contour maps constructed on top Abu Roash “G-10” and “G-20” zones, (Fig.4;5) show that the depth value reach maximum toward the southeastern part of the study area while minimum value occurred in the central part at the closure and all sedimentary sequence are dipping gradually to north direction. The area influenced by one major normal fault trending E-W (F1), (The fault tends appear to swing from WNW- to ENE but it generally East-West direction), there are five minor faults, the most important minor fault was (F2) trending NW-SE and throws dip to SW. The major fault (F1) is a southerly dipping with a maximum vertical relief of about  $\pm 800$ -1000 feet toward the east and decreasing until reach  $\pm 350$  feet to the center of the study area. The (F1) heave almost +46 meter toward the west and central part of the study area which indicate a semi-vertical fault on the other hand heave of the same fault tend to increase toward the east till reach +200 feet. The NW fault (F2) is a SW dipping minor normal fault leading to form north El Diyur area structure with a vertical relief of about  $\pm 250$  feet. These faults (F1, F2) leading to form a closures which interpreted to be a fault-dependent three-way dip closures which formed traps for the hydrocarbons on the top of Abu Roash “G-10” and “G-20” zones. Both faults trends related to dextral convergence between Africa and Eurasia, Africa and Eurasia changed from sinistral divergence to dextral convergence until the Late Cretaceous ([7]; [8]).

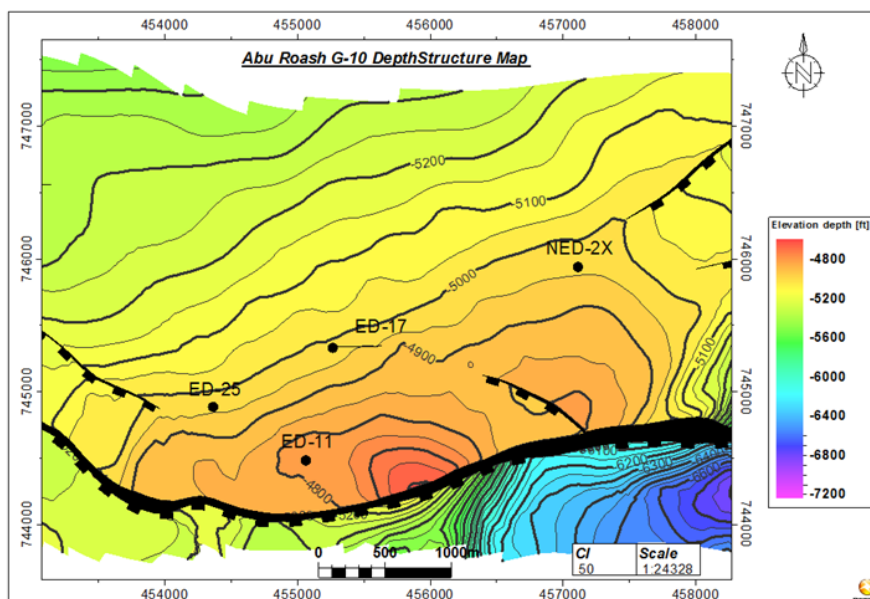


(Fig.4): Depth structure map on the top of Abu Roash “G-10” zone.

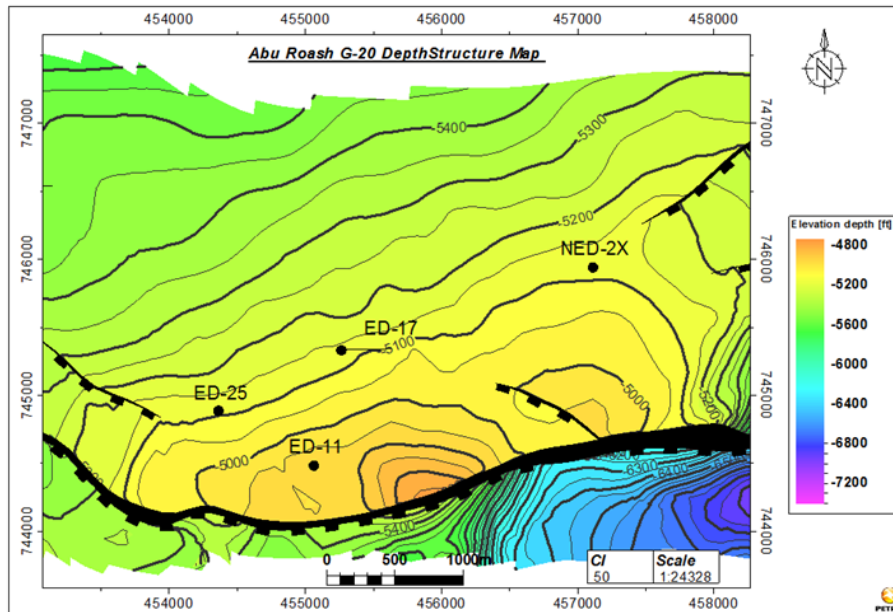


(Fig.5): Depth structure map on the top of Abu Roash "G-20" zone.

### Well Log Analysis

#### Neutron Density crossplot

Abu Roash "G-10" zone represent the middle clastic reservoir zone of Abu Roash "G" Member, (Fig.6) shows the neutron density crossplots that have been applied on the Abu Roash "G-10" zone. It is observed that, the reservoir sandstone plotted points are scattered and lay between sandstone and limestone lines with average grain density ( $p_{ma}$ ) is 2.67 gm/cc and neutron porosity ranging from 22% to 28%. The zone is mainly reservoir sandstone with non-reservoir siltstone scattered and lay between limestone and dolomite lines. (Fig.7) shows the neutron density crossplots that have been applied on the Abu Roash "G-20" sand-I zone. It is observed that, the major plotted points are scattered and lay between sandstone and limestone lines with average grain density ( $p_{ma}$ ) is 2.65 gm/cc and neutron porosity ranging from 20% to 30%. The zone is mainly sandstone with non-reservoir siltstone. While (Fig.8) shows the neutron density crossplots of Abu Roash "G-20" sand-II zone, the plotted points are scattered and lay between sandstone and limestone lines with average grain density ( $p_{ma}$ ) is 2.67 gm/cc and neutron porosity ranging from 22% to 28%. The zone is mainly calcareous sandstone with siltstone.

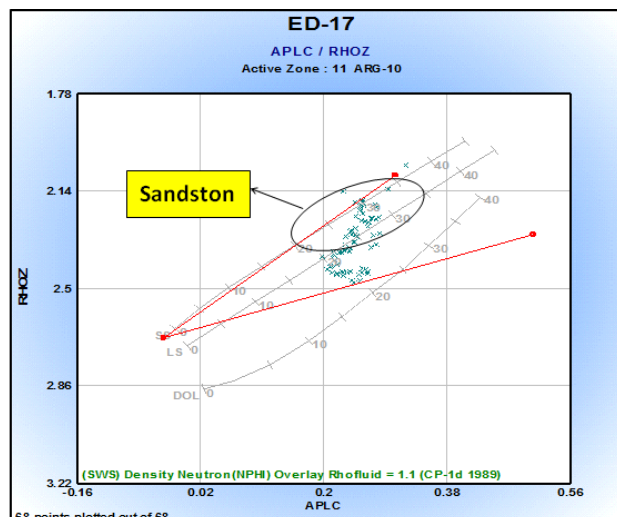


(Fig.6): Neutron density cross-plot showing the lithological components of the Abu Roash "G-10" zone.

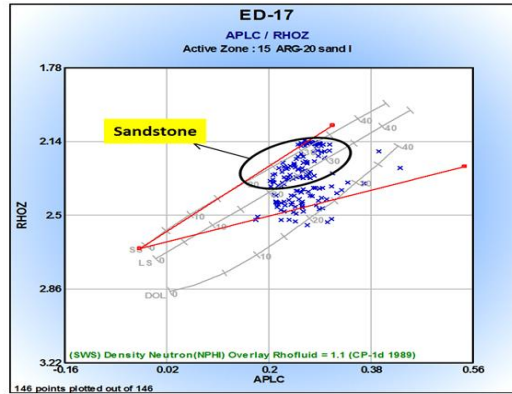


(Fig.7): Neutron density cross-plot showing the lithological components of the Abu Roash "G-20" Sand-I zone.

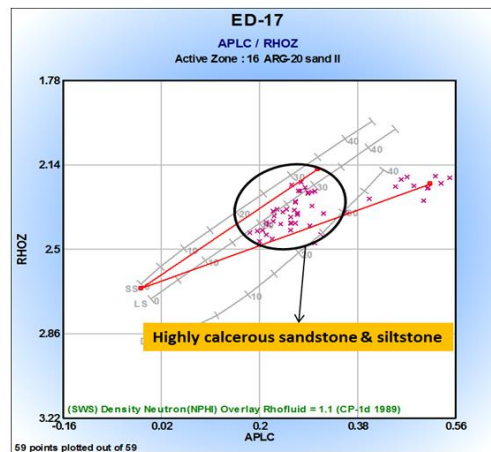


(Fig.8): Neutron density cross-plot showing the lithological components of the Abu Roash "G-20" Sand-II zone.

#### 4.2. Well log analysis results

(Table 1): Reservoir and pay summaries resulted from the petrophysical analysis.

ED-11 Reservoir Summary	Gross Interval (Feet)	Net Reservoir (Feet)	Net Reservoir/ Gross Interval (%)	Average Phi Eff. (%)	Average Sw (%)	Average Vcl (%)
ARG "10"	33	10	30	11	85	40
ARG"20"sand-I	31	28	90	23	32	16
ARG"20"sand-2	13	5	38	12	80	37
ED-11 Pay Summary	Gross Interval (Feet)	Net Pay (Feet)	Net Pay/ Gross Interval (%)	Net Pay Average Phi Eff. (%)	Net Pay Average Sw (%)	Net Pay Average Vcl (%)
ARG "10"	33	7	21	23	37	11
ARG"20"sand-1	31	28	90	24	24	13
ARG"20"sand-2	13	1	7	18	56	27
ED-17 Reservoir Summary	Gross Interval (Feet)	Net Reservoir (Feet)	Net Reservoir/ Gross Interval (%)	Average Phi Eff. (%)	Average Sw (%)	Average Vcl (%)
ARG "10"	36	19	52.7	16	66	32
ARG"20"sand-I	48	33	68.7	20	57	17
ARG"20"sand-2	22	8	36.3	18	69	30
ED-17 Pay Summary	Gross Interval (Feet)	Net Pay (Feet)	Net Pay/ Gross Interval (%)	Net Pay Average Phi Eff. (%)	Net Pay Average Sw (%)	Net Pay Average Vcl (%)
ARG "10"	36	14	38	24	39	16
ARG"20"sand-I	48	31	64.5	25	28	12
ARG"20"sand-2	22	1	12.5	23	53	24

NED-2X Reservoir Summary	Gross Interval (Feet)	Net Reservoir (Feet)	Net Reservoir/ Gross Interval (%)	Average Phi Eff. (%)	Average Sw (%)	Average Vcl (%)
ARG "10"	35	17	49	16	73	32
ARG"20"sand-I	23	18	78	19	57	24
ARG"20"sand-2	18	8	44	17	69	28
NED-2X Pay Summary	Gross Interval (Feet)	Net Pay (Feet)	Net Pay/ Gross Interval (%)	Net Pay Average Phi Eff. (%)	Net Pay Average Sw (%)	Net Pay Average Vcl (%)
ARG "10"	35	12	34	27	30	8
ARG"20"sand-I	23	15	65	22	40	14
ARG"20"sand-2	18	3	17	24	50	16

### 4.3. Lateral variation of reservoir properties

After calculating the values of the log- parameters, the values have been averaged and mapped to represent their general distribution.

#### 4.3.1. Abu Roash "G-10" zone

Abu Roash G-10 sandstones were deposited in prograding deltaic distributary environment and exhibit coarsening-upward profile with related increase in reservoir quality upwards [9]. The net reservoir sandstone isopach map of the Abu Roash "G-10" zone (Fig.9) shows an increase towards the central and western part of the study area with maximum value of (25 feet) and minimum value of (2 feet). Two sandstone bodies separated by facies barrier (non-reservoir fine sandstone and siltstone) this barrier trending northwest direction. From distribution pattern of net reservoir sandstone and the gradual upward decreasing in Gamma ray log response reflects an increasing in depositional energy upward characterized this sandstone bodies (Fig.13) Abu Roash "G-10" were deposited as a distributary river mouth bar facies ([10];[11]), on other hand the area of low values of sandstone might represent interdistributary fine sandstone and siltstone. The effective porosity distribution map of the Abu Roash "G-10" (Fig.10) shows an increase toward the central and western part of the study area and decrease toward the interdistributary fine sandstone and siltstone to the west. It reaches the maximum value (29%) at the mouth bar facies and the minimum (6%) toward the interdistributary fine sandstone and siltstone facies which reflects the effect of facies distribution on the effective porosity values. Distribution of the clay volume (Fig.11) shows an increase of clay volume toward the interdistributary fine sandstone and siltstone which reflects that clay volume was controlled by facies distribution. The water saturation distribution map of the Abu Roash "G-10" zone (Fig.12) shows an increasing toward the down-dip of the major normal fault (F1) where it reaches the maximum value (100%) The water saturation decreasing toward the up-dip of the major fault of the study area reaching the minimum value (28%).The high values of water saturation toward the up-dip of the major fault is due to facies change from sandstone to siltstone.

Both facies and structure elements were controlled the water saturation distribution of Abu Roash "G-10"zone.

#### 4.3.2. Abu Roash "G-20" zone

Abu Roash "G20" was deposited entirely in shallow marine environments where the sands exhibit strong linear trends. These sands were apparently deposited in sub-tidal bars within a marine embayment. This interval contains no evidence of incision at the base of the sands and the best sand facies exhibit current ripple cross bedding, presumably from tidal currents [9]. Abu Roash "G-20" represent the lower clastic reservoir zone of Abu Roash" Member, this zone represented by reservoir sandstone and siltstone. Abu Roash "G-20" classified into "G-20"sand-I and "G-20"sand-II zones based on the reservoir sandstone quality due to the calcareous cement of "G-20"sand-II.

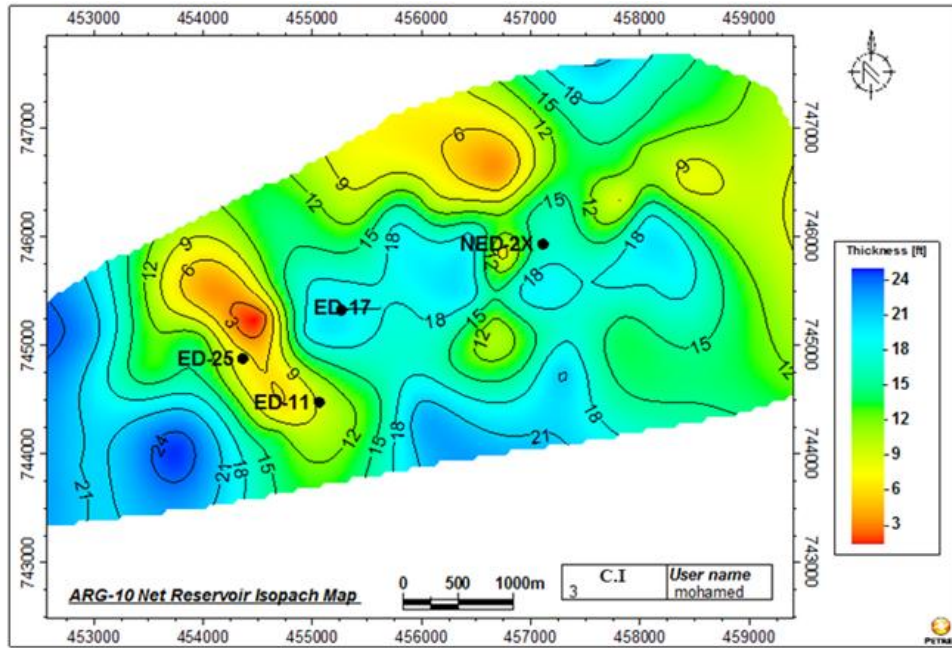


(Fig.9): Net reservoir isopach map for Abu Roash "G-10" zone.

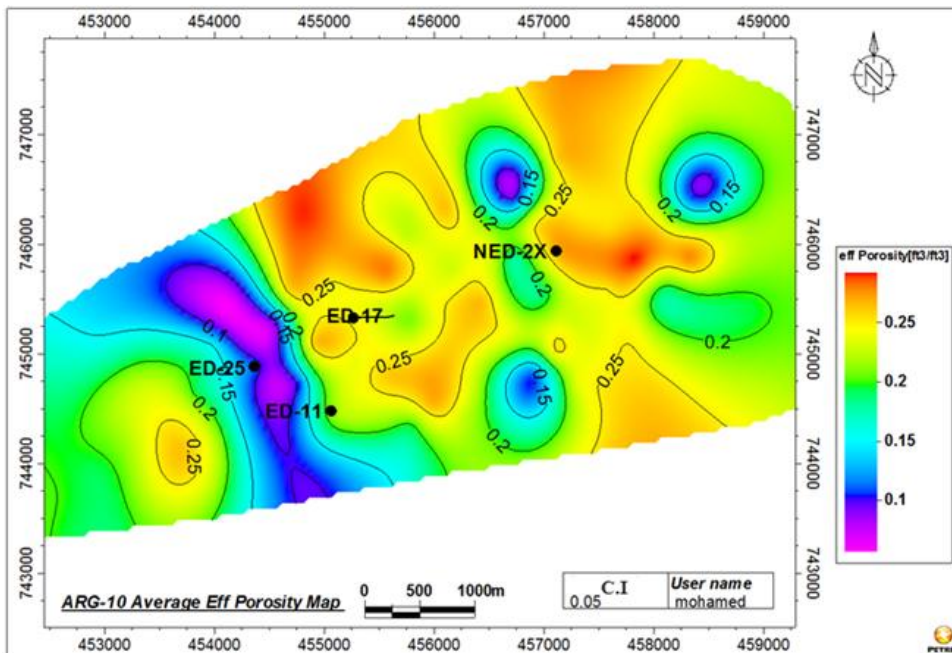


(Fig.10): Average effective porosity map for Abu Roash "G-10" zone.

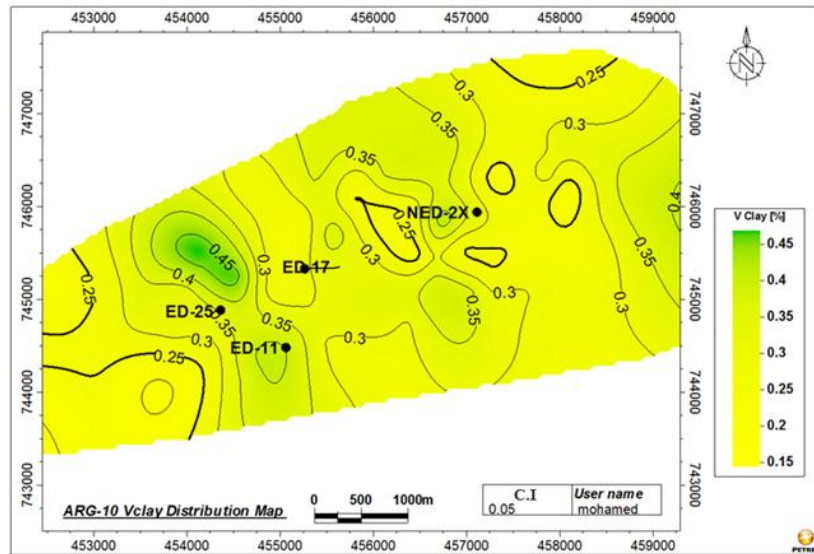


(Fig.11): Average clay volume distribution map for Abu Roash "G-10" zone.

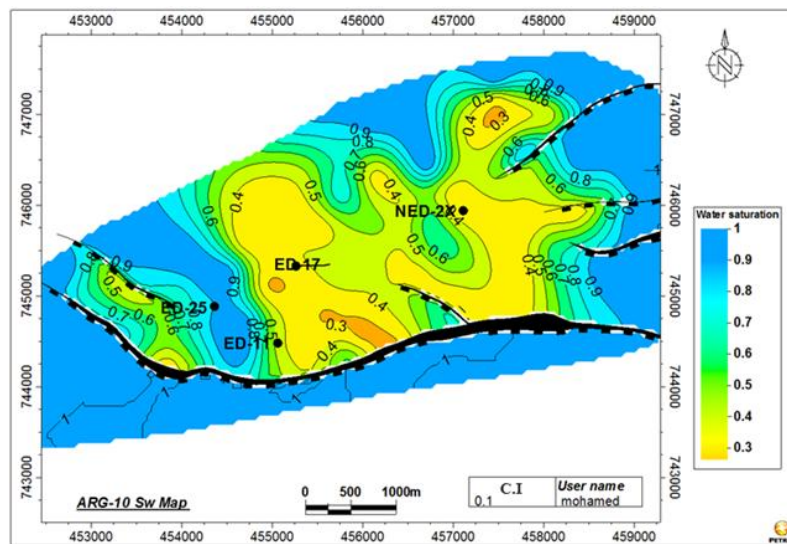


(Fig.12): Water saturation map for Abu Roash "G-10" zone.

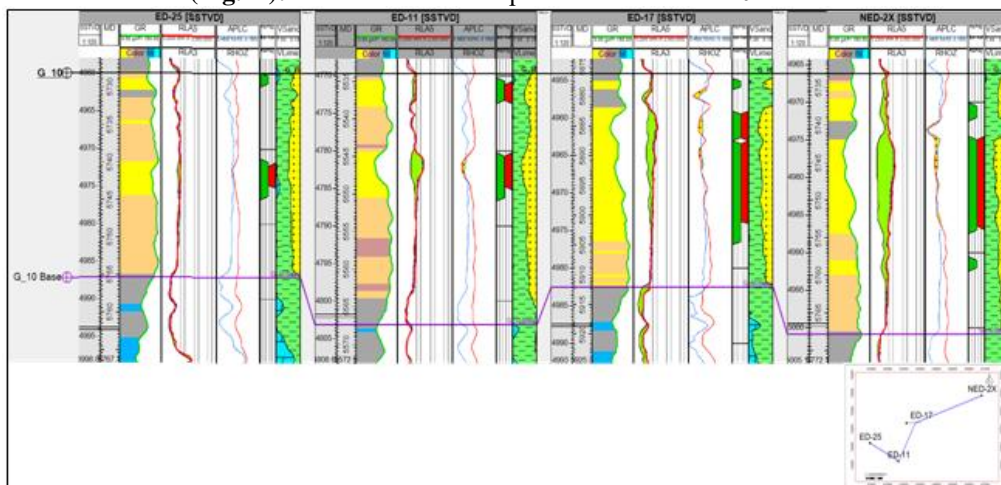


(Fig.13): Stratigraphic well-section flattened on top Abu Roash "G-10" shows the gradually upward decreasing of Gamma Ray response (sandstone coarsening upward).



#### 4.3.2.1. Abu Roash “G-20” sand-I

The net reservoir sandstone isopach map of the Abu Roash “G-20 sand-I” (Fig.14) shows an increasing on reservoir sandstone thickness towards the central part of the study area with maximum value (32 feet) at sandstone body trending to the northeast direction, and minimum value (3 feet) to the eastern part of the study area. From distribution pattern of net reservoir sandstone and the gradual upward increasing in Gamma ray log response which characterized this sandstone body (Fig.22) reflects a decreasing in depositional energy upward which characterizes the tidal creeks [10], this tidal creek cross cut the surrounded tidal flat sediments. The effective porosity distribution map (Fig.15) shows an increasing toward the central part of the study area especially toward tidal creek facies, reaches the maximum value (23%) which reflects the influences of facies distribution on effective porosity and decrease toward the east and western part it reaches the minimum value (11 %) toward the east. The clay volume distribution map (Fig.16) shows an increasing toward the eastern part of the study area. The water saturation distribution map (Fig.17) shows that the water saturation decreasing toward the up-dip of the major normal fault (F1) reaching the minimum value (32%), and increasing toward the down-dip of the major normal fault (F1) where it reaches the maximum value (100%). Water saturation distribution was controlled by the structure elements.

#### 4.3.2.2. Abu Roash “G20” sand-II

The net reservoir isopach map of the Abu Roash “G-20” sand-II (Fig.18) shows an increasing on reservoir sandstone thickness towards the eastern and central part of the study area with maximum value (13 feet) and minimum value (3 feet) to the south western part of the study area. The effective porosity distribution map (Fig.19) shows an increasing in the effective porosity toward eastern and central part of the study area, reaches the maximum value (21%) and decrease toward the southern part, and reaches the minimum value (9 %), the distribution of effective porosity reflects that effective porosity was controlled by sandstone distribution. The clay volume distribution map (Fig.20) shows an increasing of the clay volume values toward the southeastern part of the study area represent the lowest values of reservoir sandstone which reflects that clay volume controlled by facies distribution. The water saturation distribution map (Fig.21) shows that the water saturation decreasing toward the up-dip of the major normal fault (F1) reaching the minimum value (46%), and increasing toward the down-dip of the major normal fault (F1) where it reaches the maximum value (100%). Water saturation distribution was controlled by the structure elements.

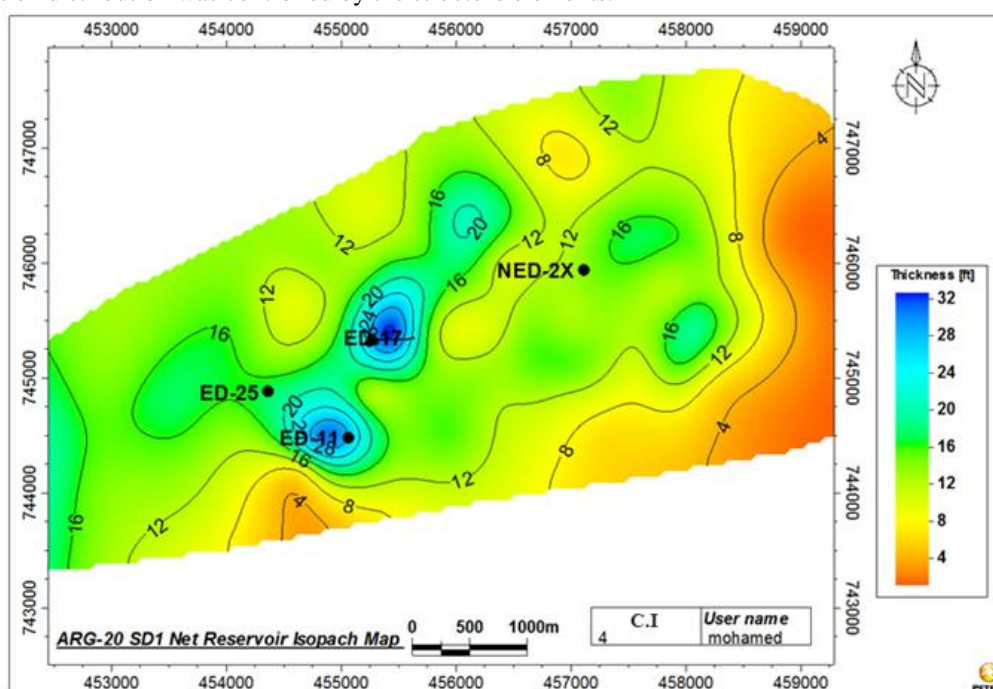


(Fig.14): Net reservoir isopach map for Abu Roash “G-20” Sand-I zone.

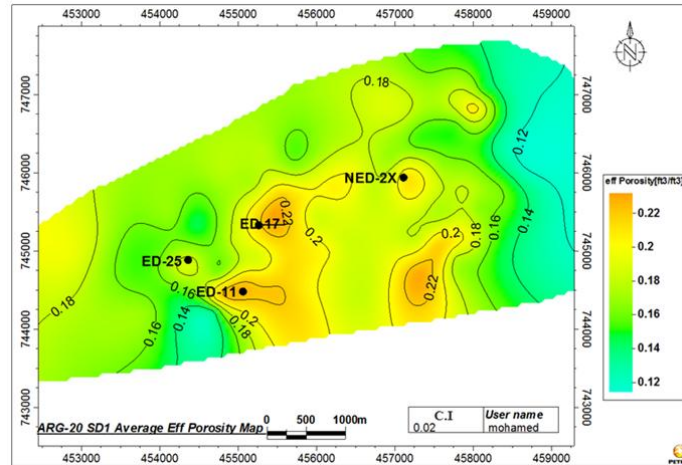


(Fig.25): Average effective porosity map for Abu Roash "G-20" sand-I zone.

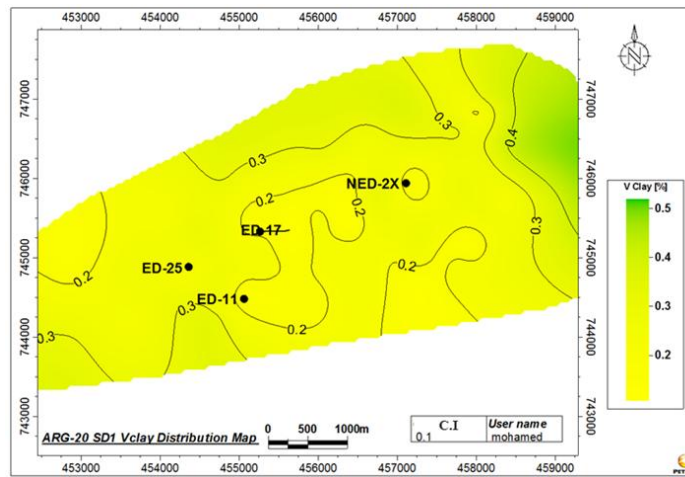


(Fig.16): Average clay volume distribution map for Abu Roash "G-20" sand-I zone.

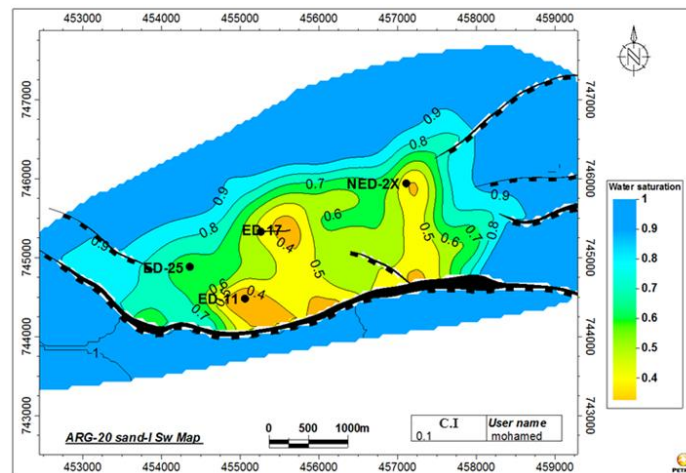


(Fig.17): Water saturation map for Abu Roash "G-20" sand-I zone.

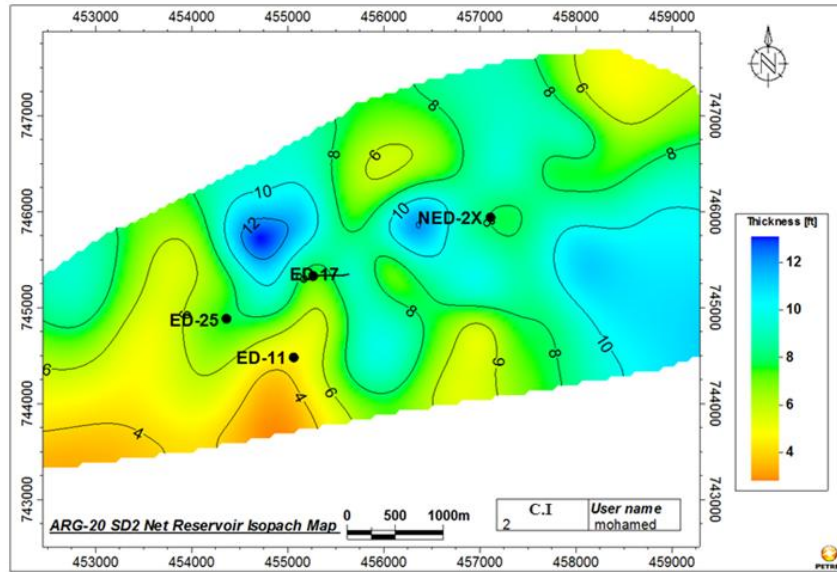


(Fig.18): Net reservoir Isopach map for Abu Roash "G-20" sand-II zone.

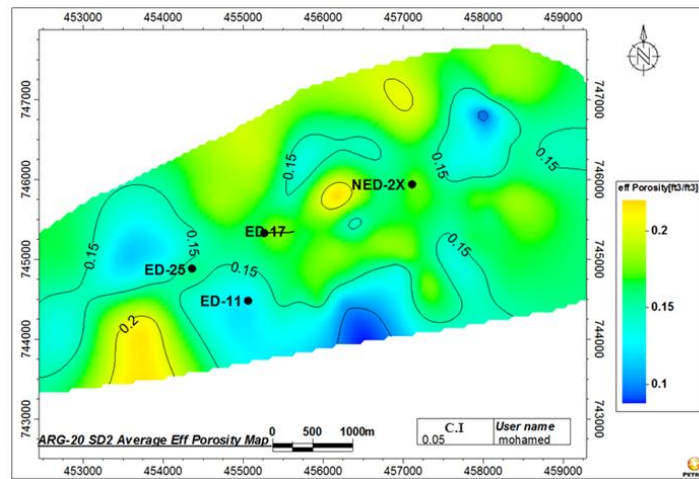


(Fig.19): Average effective porosity map for Abu Roash "G-20" sand-II zone.

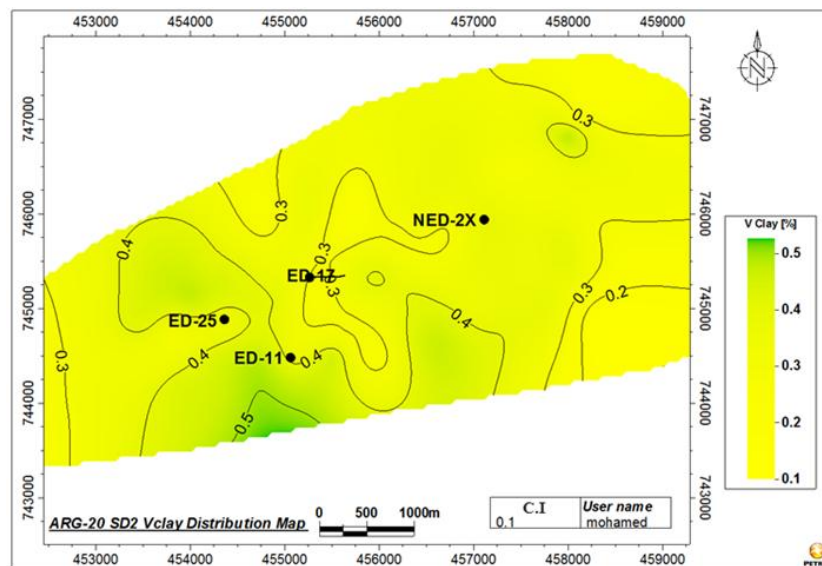


(Fig.20): Average clay volume distribution map for Abu Roash "G-20" sand-II zone.

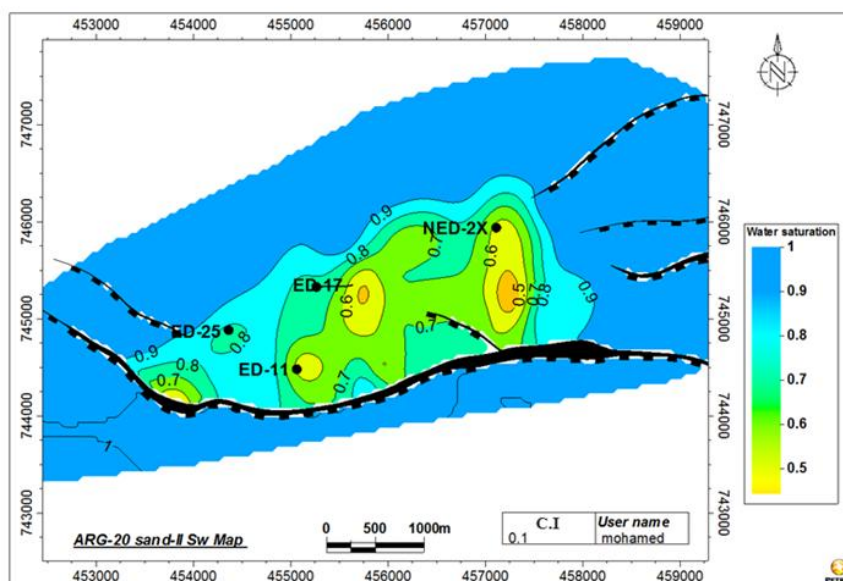


(Fig.21): Water saturation distribution map for Abu Roash "G-20" sand-II zone.

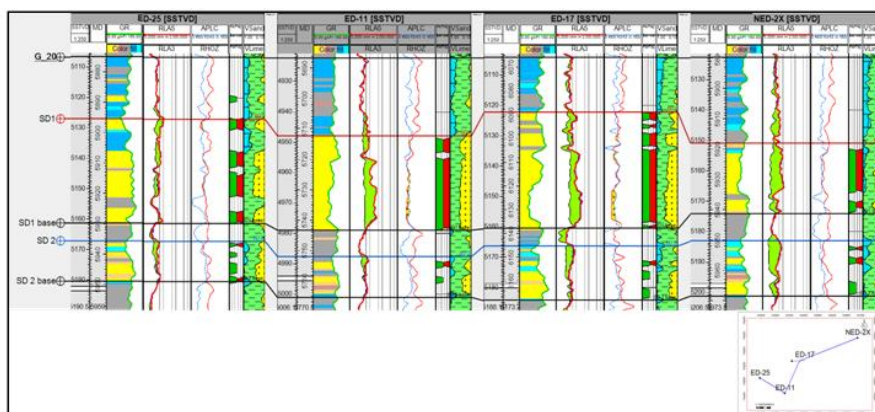


(Fig.22): Stratigraphic well-section flattened on top Abu Roash "G-20" shows the fining upward of Gamma Ray log response of ED-11 and ED-17 wells "tidal creek" and normal tidal flat sandstone and siltstone of ED-25 well.

### Hydrocarbons Volume calculation

Preliminary hydrocarbon volumes have been estimated for "G-10" and "G-20" reservoir zones. The reservoir input parameters were based on the sums and averages from the first four drilled wells penetrating the reservoir section. These estimation were calculated based upon the following formula expressed in terms of stock tank of original oil in place (STOOIP):  $STOOIP (STB) = 7758 * A * h * \Phi_{eff} * (1-S_w) * N/G * 1/B_o$  Where, A= reservoir area in acre, h= netpay thickness in feet,  $\Phi_{eff}$  =effective porosity in fraction,  $(1-S_w)$  = hydrocarbon saturation in fraction, N/G = net to gross reservoir ratio,  $B_o$  = formation volume factor and 7758 is an acre feet conversion for oil.

(Table 2): The stock tank of original oil in place STOOIP estimated for zones

Zone	STOOIP MMSTB
Abu Roash G-10	53
Abu Roash G-20 Sand-I	38
Abu Roash G-20 Sand-II	13.6

### III. Summary and Conclusions

The principal structure responsible for hydrocarbon entrapment in the study area was a structural high which correspond to the three way dip closure of East-West major normal fault (F1) and the Northwest-Southeast normal fault of North El Diyur area (F2).

Abu Roash "G-10" zone consist of sandstone were deposited as distributary river mouth bar and interdistributary fine sandstone graded to siltstone with net reservoir thickness between (max. 25 feet - min. 2 feet), effective porosity reaches (max. 29% - min. 6%) at the mouth bar facies and the interdistributary fine sandstone and siltstone respectively, water saturation values ranging between (max. 100% - min. 28%), water saturation was controlled by structural and facies elements while effective porosity and clay volume were controlled mainly by facies distribution. Abu Roash "G-20 sand-I" consist of sandstone deposited at tidal flat environment with net reservoir thickness between (max. 33 feet - min. 3 feet), effective porosity reaches (max. 23% - min. 11%) at tidal creek sandstone facies and fine tidal flat sandstone respectively. Water saturation values ranging between (max. 100% - min. 32%). Abu Roash "G-20 sand-II" reservoir composed of calcareous sandstone with net reservoir thickness between (max. 13 feet - min. 3 feet), effective porosity reaches (max. 21% - min. 9%), water saturation values ranging between (max. 100% - min. 46%). Water saturation values were controlled by structural elements while effective porosity and clay volume controlled mainly by facies distribution at Abu Roash "G-20" Sand-I & Sand-II. The cumulative stock tank of original oil in place STOOIP estimated for the three zones is 104.6 Million Stock Tank Barrel

### Acknowledgement

A word of gratitude is extended to the Egyptian Petroleum Corporation (EGPC), Qarun Petroleum Company (QPC). Sincere thanks to all the staff of Al-Azhar University.

### References

- [1]. Schlumberger, Geology of Egypt Paper presented at the Well Evaluation Conference, Schlumberger, Cairo. (1995), pp. 58-66.
- [2]. Hantar, G, North Western Desert, In Said, R. (1990), Geology of Egypt, (A.A. Balkema, Rotterdam, Brookfield, 1990) pp.293-320.
- [3]. Abdel Aal, A, Subsurface study of the Abu Gharadig basin, Western Desert, Egypt, Msc. Thesis, Ain Shams University, (1990)
- [4]. Fawzy, A., and Dahi, M, Regional geological evaluation of the Western Desert, Egypt: Paper presented at the Geology of the Arab World, Cairo University, 1992, pp.111-149.
- [5]. Moustafa.A. R., Mesozoic-Cenozoic Basin Evolution in the Northern Western Desert of Egypt. Geology of East Libya, vol. 3, 2008, pp. 35-42.
- [6]. W. M. Meshref, Tectonic framework of Egypt. In Said, R. (Ed.), Geology of Egypt, 1990, 113-156, Balkema, Rotterdam
- [7]. Savostin, L.A., Sibuet, J.-C., Zonenshain, L.P., Le Pichon, X., and Roulet, M.-J., "Kinematic evolution of the Tethys belt from the Atlantic Ocean to the Pamirs since the Triassic Tectonophysics", v. 123, (1986).
- [8]. Smith, A.G, Alpine deformation and the oceanic area of Tethys, Mediterranean and Atlantic. Bull. Geol. Soc. Am. 82, 1971, 2039-2070.
- [9]. Pasley, M.A., Gabe Artigas, and Nassef, Osama and Joe Comisky, Depositional Facies Control on Reservoir Characteristics in the Middle and Lower Abu Roash "G" Sandstones, Western Desert, Egypt. Adapted from oral presentation at AAPG International Conference and Exhibition, Cape Town, South Africa, October 26-29, 2008.
- [10]. Cant, D.J., Subsurface facies analysis, in Walker, R.G., and James, N. P. eds., facies models: response to sea level change, Geological association of Canada, St. Johns, Newfoundland, 1992, P 27-45.
- [11]. Coleman, J.M., & prior, D.B, Deltaic environment in sandstone depositional environments. AAPG, Mem. 31, (1982).